Low-temperature properties of monoclinic pyrrhotite

Poster · December 2016

DOI: 10.13140/RG.2.2.27090.76483

2 authors:

Michael Volk
Harvard University

Stuart Gilder
Ludwig-Maximilians-University of Munich

Low temperature magnetic properties of monoclinic pyrrhotite
with particular relevance to the Besnus transition

Michael Volk[1], Stuart Gilder[1], Joshua Feinberg[2]

[1]Ludwig Maximilans Universität, München Germany

[2]Institute for Rock Magnetism, University of Minnesota, Minneapolis

LUDWIG-MAXIMILIANS-UNIVERSITÄT MÜNCHEN

planetary magnetism

Introduction

Pyrrhotite refers to a group of non-stoichiometric iron sulfides, $Fe_{1-x}S$ with $0.08 < x < 0.125$, that are important carriers of magnetic remanence in some terrestrial and extraterrestrial rocks. It is especially important as the main magnetic carrier in some Martian meteorites.

Alternating layers of ordered vacancies in the iron layers lead to different superstructures [1]. The most iron deficient 4C pyrrhotite (Fe_7S_8) is ferromagnetic. It undergoes the "Besnus transition" at $T_{Bes} \approx 30K$, which is not well understood.

Meteorites at the outer edge of the meteorite belt can cool to T ≈ 120-150K [2].

How much of the natural remanence is lost by cooling in space and warming to room temperature?

Paleointensities from meteorites are usually determined with the REM method, where:

$$B_{pal} = REM \times 3000 = (NRM / SIRM) \times 3000$$

If the NRM decreases by low temperature demagnetization,

What is the influence on paleointensity recording?

Samples

Pyrrhotite-bearing gneiss samples (P167, P512 and P527, $T_c = 319 \pm 5$ °C) from the Black Forest, Germany

A pure polycrystalline pyrrhotite sample (MSM73410, $T_c = 320$ °C) from Schmiedeberg, Germany

An oriented (with EBSD) monoclinic pyrrhotite single crystal disc (sample MSM17591) to study the Besnus transition ($T_c = 318$ °C)

The samples don't show any sign of a λ-transition where hexagonal pyrrhotite transforms into monoclinic pyrrhotite. Curie temperatures lie within literature values -> pure monoclinic.

Methods & Results

Curie temperatures were measured with a variable field translation balance (VFTB). Low temperature measurements, hysteresis loops and backfield curves were measured to maximum fields of 1.5 T with a Princeton Measurements Corporation vibrating sample magnetometer (VSM) at the University of Munich and the University of Minnesota (IRM).

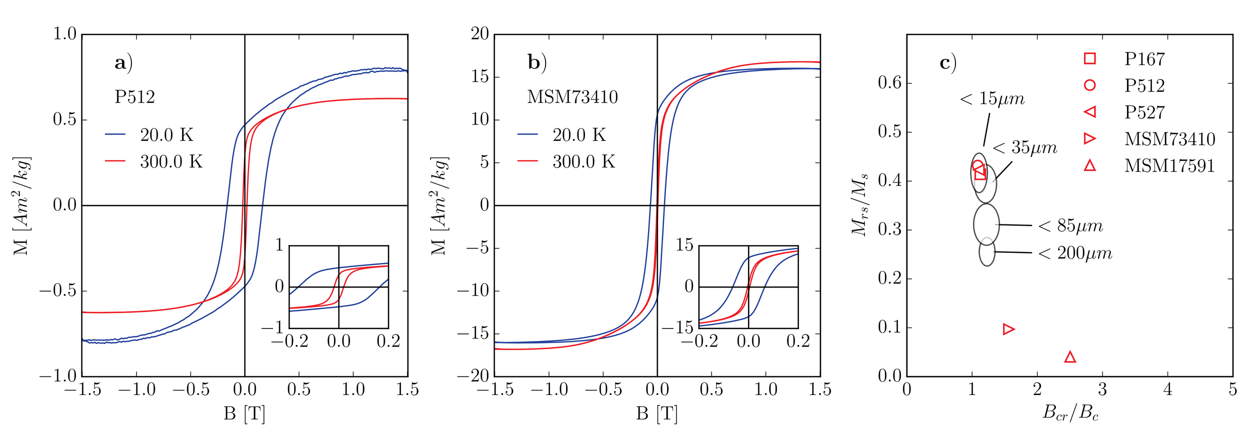

Fig. 1: Hysteresis loops of a) rock sample containing monoclinic pyrrhotite, b) large crystal of monoclinic pyrrhotite. c) Day plot for all samples used in the study. Circles show the mean and one standard deviation for grain size fractions from Dekkers et. al (1989)

Rock samples have remanence ratios ≈0.4 and coercivity ratios (<1.5) typical of PSD pyrrhotite with grain sizes <35 μm. MSM73410 and MSM17591 have lower M_{rs}/M_s and higher B_{cr}/B_c characteristic of MD pyrrhotite with grain sizes >200 μm.

Continuous thermal demagnetization

The samples were given a 1 T room temperature ($T_r = 300$ K) isothermal remanent magnetization (IRM) and then cycled from T_r to T_i ($T_i \approx$ 200, 150, 120, 90, 60, 40, 30 and 20 K) and then warmed back to T_r.

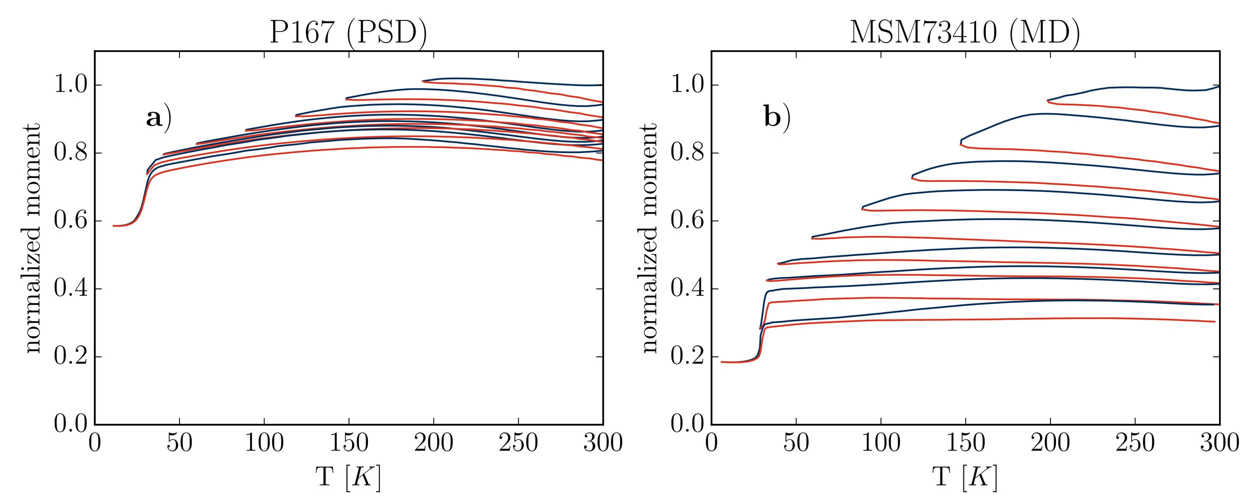

Fig 2: Continuous demagnetization of a strong field (1 T) saturating isothermal remanent magnetization to reversal temperatures T_i. (Princeton - VSM)

PSD-dominated samples show significantly less relative loss in magnetization upon low-temperature cycling than MD samples (Fig. 2). The greatest loss in remanence occurs at the Besnus transition.

In contrast to magnetite, the cooling paths do not trace the warming path of the previous cycle.

Stepwise Thermal demagnetization

Stepwise demagnetization is calculated from the continuous demagnetization as the remaining fraction of IRM after cycling from $T_r \rightarrow T_i \rightarrow T_r$ as a function of T_i.

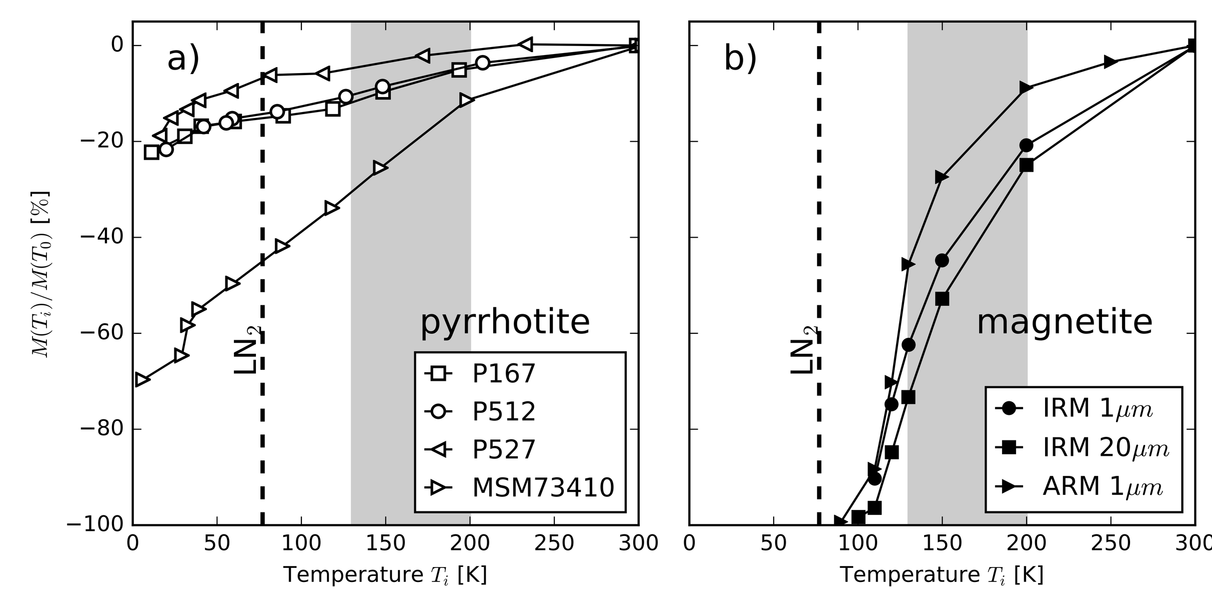

Fig 3: Stepwise thermal demagnetization of a) pyrrhotite calculated from continuous demagnetizations (Fig. 2) and b) magnetite (data from Dunlop [2003].

The magnetization loss for $T_i > T_{Bes}$ for the PSD samples averages −7 % / 100 K, whereas that for the MD sample is roughly four times steeper −27.8 %/100 K.

Single Crystal Low temperature behavior

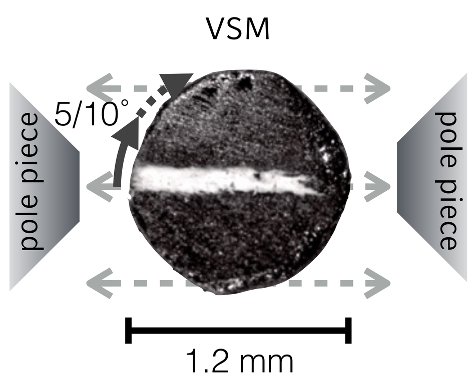

Fig. 4: Sketch of sample position inside pole pieces of the VSM.

A disk was drilled from a single crystal and oriented using electron backscatter diffraction. The c-axis of the single pyrrhotite is oriented almost normal (77°) to the sample's surface. The a_1 axis is arbitrarily defined as one of the a-axes ($a_1 = 0°$, $a_2 = 57°$ and $a_3 = 116°$ with respect to a_1).

Hysteresis loops were measured every 5° and backfield curves every 10° in the basal plane of the single crystal at 300 K and every 2 K from 50 K through the Besnus transition until 20 K.

Magnetic behaviour above T_{Bes} (>34 K)

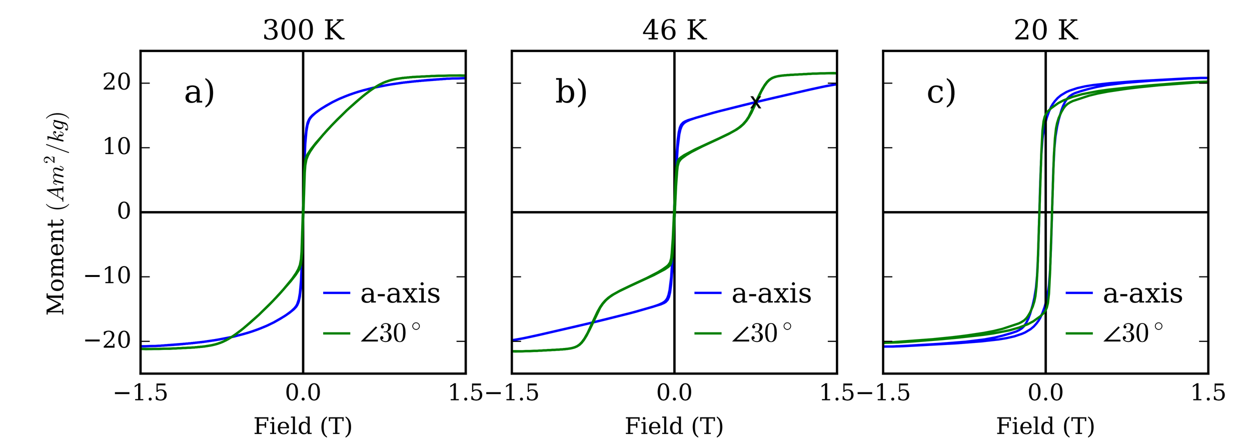

Fig. 5: Hysteresis loops along an a-axis and 30° to a-axis. b) shows second inflection that disappears at $T<T_{Bes}$

Shallow approach to saturation, crystal not fully saturated at 300 K in 1.5 T ($M_s^* = 21.2$ Am^2/kg). M_s^* shows six fold symmetry (Fig. 6a).

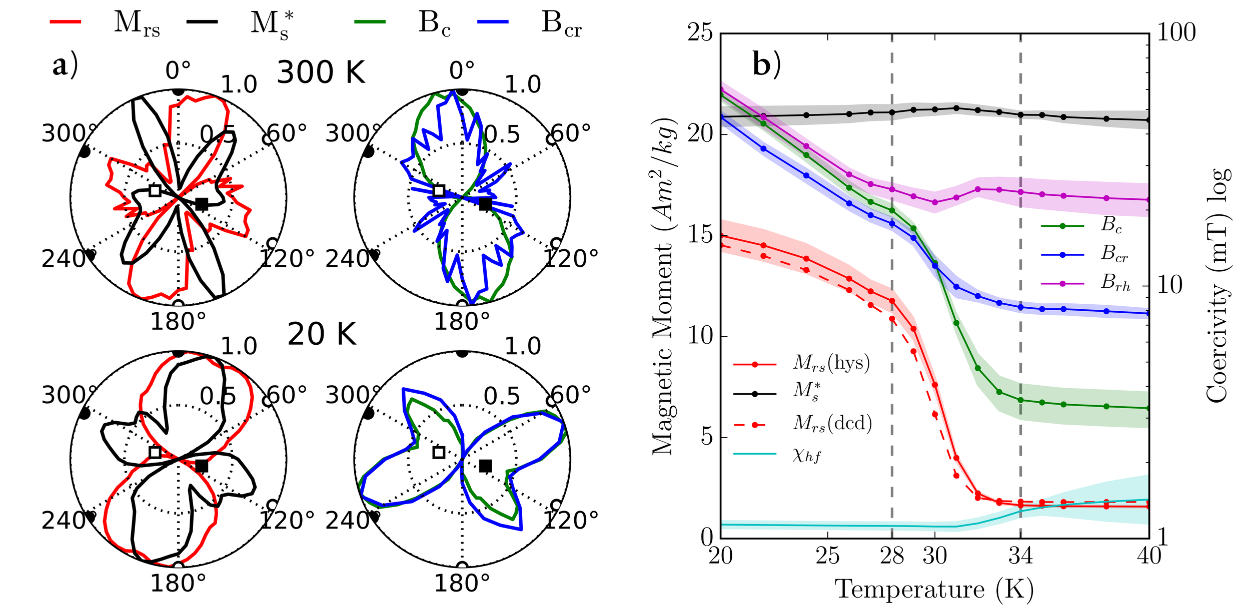

Fig 6: Rock magnetic parameters as a **left:** function of angle normalized to *1 = max, 0 = min.* Circles show a-axes. **right:** as a function of temperature. Mean over all directions with one standard deviation (shaded). Dashed line as determined from backfield (dcd).

A second inflection appears at temperatures (< 200 K) when measured in-between crystallographic a-axes (Fig. 8). The closer the measurement direction is to an a-axis, the higher the field at which the inflection appears (B_{inf}) and the less pronounced it becomes. Onset of second inflection (Fig. 7) at T < 200 K, coinciding with the maximum of K_4 and a change in sign of K_3 anisotropy constants [Bin and Pauthenet, 1963].

Magnetic behaviour within T_{Bes}(34–28 K)

Drastic increase in coercivity and saturation remanence (Fig. 6b), with $B_{cr} < B_c$ at T < 30 K. Mean saturation magnetization stays constant over all temperatures.

Second inflection starts to disappear with the inflection field moving towards lower fields.

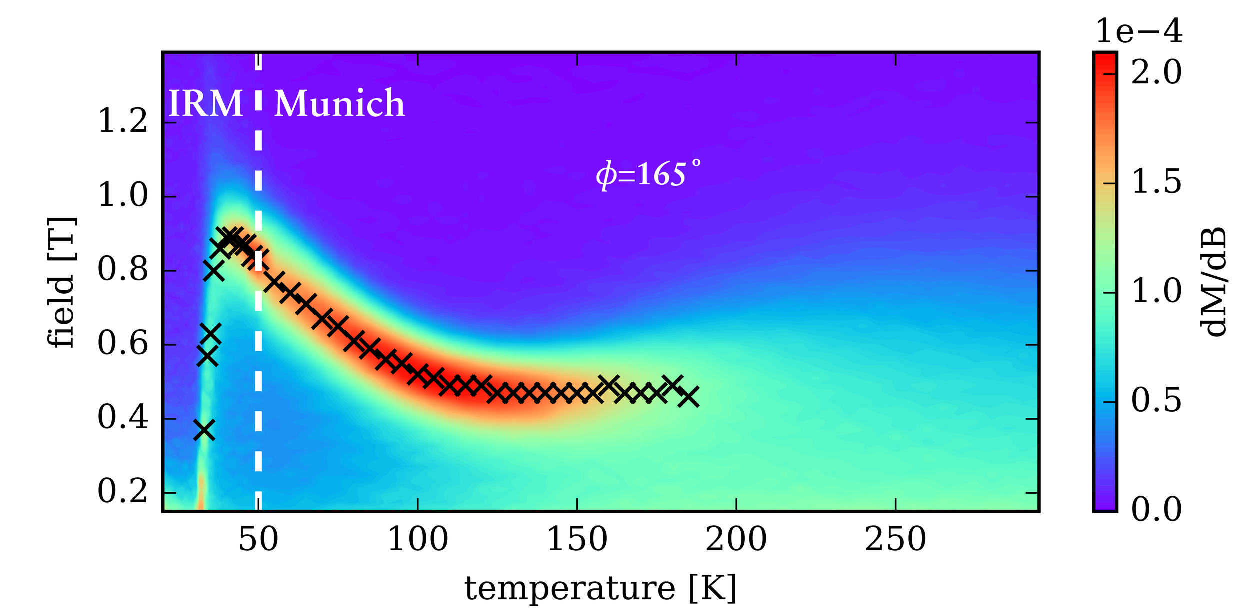

Fig. 7: First derivative (dM/dB) of the 165° downfield branch of the hysteresis measurements (B>0). Red patches show the appearance of the second inflection. Crosses mark the maximum of the first derivative.

Magnetic behaviour below T_{Bes} (< 28 K)

Symmetry of saturation magnetization M_s^* changes from 6 fold at T > 34 K to 4 fold while coercivities change from 2 fold to 4 fold symmetry below T_{Bes} (Fig. 6).

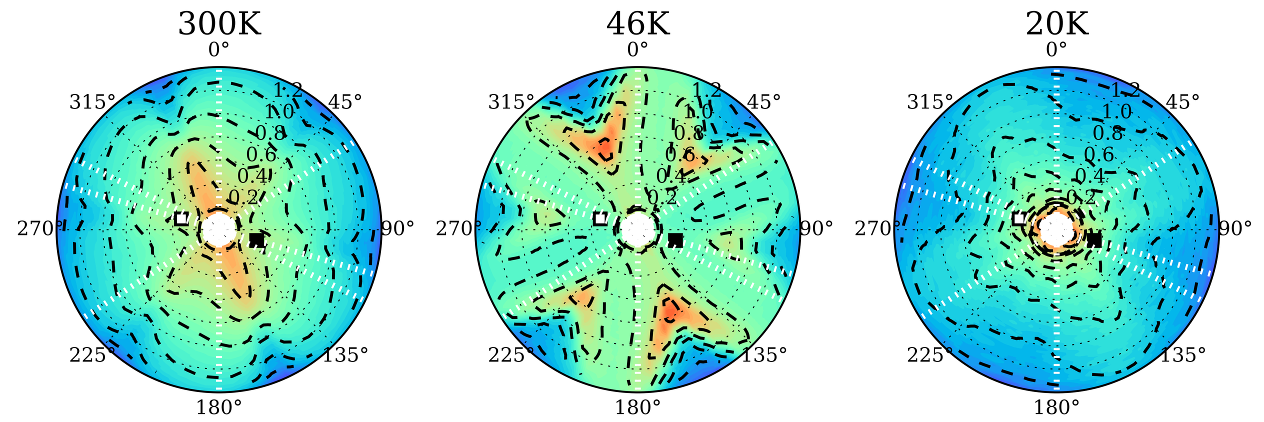

Fig. 8: Angular dependence of the first derivative of the ascending branches of the hysteresis loops. Radial distance corresponds to the field value in T, as indicated by the labeled black dashed lines. The central area (B < 30 mT) was omitted for clarity. White dashed lines indicate the crystallographic a-axes. White line with square represent the c-axis and its projection on the basal plane. A hexagonal pattern is present in the data between 50 and 34 K with the second inflections aligned between a-axes.

Second inflection disappeared completely with derivatives showing 4 fold symmetry.

Conclusions

- NRM lowered by 5-10 % for PSD and 20-40 % for MD samples. Low temperature cycling has a much stronger effect on magnetite (Dunlop, 2003).
- Compared to uncertainties of REM method low temperature demagnetization of remanence in pyrrhotite is small.

Paleointensities from pyrrhotite-bearing meteorites are slightly influenced by temperature cycling in space

- Second inflection appears at T ≈ 200 K (B_{inf} = 470 mT) where K_4 is max and K_3 changes sign with maximum at T = 40 K, B_{inf} = 890 mT and disappears at T_{Besnus}.
- Second inflection shows a six fold symmetry, linked to the crystal structure (between a-axes).
- Possible explanation for second inflection is a field induced switching of easy axes as proposed by Bin & Pauthenet (1963).
- Second inflection & M_s^* show a symmetry change from six fold at $T>T_{Besnus}$ to four fold $T< T_{Besnus}$.
- Data supports a change from hexagonal [6x] -> triclinic [4x] as proposed by Wolfers (2011).

References

[1] Morimoto, N., et al., 1970. Pyrrhotites: stoichiometric compounds with composition $Fe_{n-1}S_n$ (n≥8), Science, 168(3934), 964–966.
[2] Weiss, B. et al. "Paleomagnetic Records of Meteorites and Early Planetesimal Differentiation." Space Science Reviews 152.1-4 (2009): 341–390
[3] Dekkers, Marinus J. "Magnetic Properties of Natural Pyrrhotite. II. High- and Low-Temperature Behaviour of Jrs and TRM as Function of Grain Size." Physics of the Earth and Planetary Interiors 57.3-4 (1989): 266–283.
[4] Dunlop, David J. "Stepwise and Continuous Low-Temperature Demagnetization." Geophysical Research Letters 30.11 (2003): 1582–4.
[5] Koulialias, D et al. "Variable Defect Structures Cause the Magnetic Low-Temperature Transition in Natural Monoclinic Pyrrhotite." Geophysical Journal International 204.2 (2016): 961–967.
[5] Bin, M, and R Pauthenet. "Magnetic Anisotropy in Pyrrhotite." Journal of Applied Physics 34.4 (1963): 1161
[6] Wolfers, Pierre et al. "The Pyrrhotite 32 K Magnetic Transition." Solid State Phenomena 170 (2011): 174–179.

published as: Volk, Gilder, and Feinberg. "Low temperature magnetic properties of monoclinic pyrrhotite with particular relevance to the Besnus transition." *Geophysical Journal International* (2016)

Michael Volk
Department für Geo- und Umweltwissenschaften
Theresienstr. 41 • 80333 Munich • Germany
email: volk@geophysik.uni-muenchen.de Tel: +49 (89) 2180-4236